Applied Energy 111 (2013) 129–141

Contents lists available at SciVerse ScienceDirect

Applied Energy

journal homepage: www.elsevier.com/locate/apenergy

Modelling of tar formation and evolution for biomass gasification: A review

Carolina Font Palma *

School of Chemical Engineering and Analytical Science, The Mill, University of Manchester, Oxford Road, Manchester M13 9PL, UK

HIGHLIGHTS

- Review of mechanisms for tar formation and evolution during biomass gasification.
- Identification of pyrolysis products from cellulose, hemicellulose and lignin.
- Identification of common use tar model compounds and their experimental and modelling study.

ARTICLE INFO

Article history:
Received 13 December 2012
Received in revised form 11 March 2013
Accepted 29 April 2013
Available online 24 May 2013

Keywords:
Tar formation
Lignin
Mechanism
Biomass
Gasification
Cellulose

ABSTRACT

Many by-products are generated during gasification, such as tar, NO_x, SO_2, and fly ash. In particular, tar elimination from the product gas is necessary to make gasification an attractive option. The presence of tar can cause operational problems to further equipment; heavy tars may condense on cooler surfaces downstream which can lead to blockage of particle filters and fuel lines. With the aim of establishing a mechanism for tar formation, tar precursors were identified based on biomass main components – lignin, cellulose and hemicellulose. This review describes the fundamentals of the possible mechanisms for tar formation and evolution, as well as the background for the development of a model for the simulation of a biomass fluidised bed gasifier.

Contents

* Present address: Energy Technology & Innovation Initiative (ETII), University of Leeds, Leeds LS2 9JT, UK. Tel.: +44 (0) 113 343 9010.
E-mail addresses: C.FontPalma@leeds.ac.uk, c.fontpalma@gmail.com

0306-2619/$ - see front matter © 2013 Elsevier Ltd. All rights reserved.
http://dx.doi.org/10.1016/j.apenergy.2013.04.082

1. Introduction

Increasing interest to substitute fossil fuels and reduce greenhouse gas emissions has promoted research on the use of biomass and agricultural waste in energy conversion processes. A technological option that has the potential to become one answer for renewable energy generation is biomass gasification. Even though coal gasification is a well-established technology, its adaptation to biomass gasification poses challenges in the designing of the process. The main reason is the chemical and physical differences between biomass and coal [1]. That is, biomass is characterised by lower fixed carbon, and higher moisture and volatile matter contents than coal.

During gasification many by-products are generated such as NO_x, SO_2, fly ash and tar. In particular, tar formation is one of the major issues to be solved when implementing this technology. The higher volatile matter makes biomass more susceptible to tar formation. Tar is a complex mixture of condensable hydrocarbons comprising single-ring to 5-ring aromatic compounds plus other oxygen-containing hydrocarbons and complex polyaromatic hydrocarbons (PAHs) [2].

The success of biomass gasification requires a reliable system that delivers a quality product. The presence of tar can cause operational problems because of the possible formation of aerosols, soot formation due to repolymerisation, and interaction of tar with other contaminants on fine particles. In addition, heavy tars may condense on cooler surfaces downstream which can lead to blockage of particle filters and fuel lines. Therefore, tar elimination from the product gas is the ultimate goal to make gasification an attractive option.

Methods to reduce and control tar formation during biomass gasification have been divided in primary methods – when the tar is removed inside the gasifier-, and secondary methods – when tar is removed in a separate step after gasification [2]. Primary methods include the appropriate selection of operating parameters, the proper design of the gasifier and the use of suitable bed additives or catalysts during gasification. In contrast, secondary methods comprise tar cracking either thermally or catalytically, or mechanical methods such as the use of cyclones and electrostatic filters. Tar reduction methods have also been categorised in five groups: mechanism methods, self-modification, thermal cracking, catalyst cracking, and plasma methods [3].

Mechanical methods are classified into two types: dry and wet gas cleaning. Dry gas cleaning methods include cyclones, rotating particle separators (RPS), fabric filters, ceramic filters, activated carbon based adsorbers, and sand bed filters which can be used to capture tar from product gas. Wet gas cleaning methods are used after gas cooling at about 20–60 °C; some examples are wet electrostatic precipitators, wet scrubbers, and wet cyclones. However, disadvantages of wet gas cleaning are that synthesis gas has to be cooled down and waste water treatment is required [4].

Self-modification methods comprise the best selection of type of gasifier and operating parameters, such as temperature, equivalence ratio (ER), the type of biomass, pressure, gasifying medium and residence time. Increases of operating temperature have shown to reduce the total number of detectable tars but favoured the formation of aromatics without substituent groups (such as benzene and naphthalene) [5]. Tar yield and tar oxygen-containing compounds decreased drastically with increases of ER. Experimental work in a fluidised bed gasifier with tree chips showed that raising the pressure from 8 to 21 bars reduced oxygenated components, and particularly phenols were almost completely eliminated, conversely, the PAH fraction increased [6].

Thermal cracking involves conversion or cracking of tar into lighter gases using high temperatures for certain residence time. It was reported for biomass tars, that the maximum quantity of tar was reached at about 773 K and then dropped with increasing temperature. At temperatures >873 K, secondary reactions (i.e. tar cracking) occurred, increasing the amount of non-condensable gases, which improved the energetic content of the product gas [7]. In addition, at least a temperature of 1523 K and residence time of 0.5 s were identified as needed to achieve high tar cracking efficiencies [3]. For catalytic cracking techniques, catalysts commonly employed are classified into six groups: nickel-based catalysts, non-nickel metal catalysts, alkali metal catalysts, basic catalysts, acid catalysts, and activated carbon catalysts [4]. Lastly, the plasma method has been used to simultaneously remove tars and particles; 50% removal of naphthalene was achieved with a corona discharge using an energy density of 40 J/L at 400 °C in about 3 min [8]. Devi et al. [2] and Han and Kim [3] have comprehensively reviewed tar reduction methods, interested readers should refer to those reports.

Tar is often classified according to its appearance as primary, secondary and tertiary tars. Primary tars have been identified as consisting of mainly oxygenated compounds produced at 673–973 K. Secondary tars are produced at around 973–1123 K and comprise phenolics and olefins; whilst tertiary tars are formed at temperatures around 1123–1273 K and consist of complex aromatic compounds [9]. As part of the tertiary tars, aromatics such as PAHs are found. Other tar classification is based on the molecular weight of tar compounds, which are divided by classes: class 1 refers to GC-undetectable tars, like heaviest tars that condense at high temperatures even at low concentrations; class 2 refers to heterocyclic compounds that generally have high water solubility, such as phenol and cresol; class 3 includes 1-ring aromatic compounds, e.g. xylene and toluene; class 4 refers to 2–3 ring PAH compounds, such as naphthalene and phenanthrene; and, class 5 includes higher PAH compounds, that is, 4–7 ring aromatic compounds from fluoranthene to coronene [3]. Another description for tar, based on tar sampling and analysis, is gravimetric tar. It refers to numerous individual tar compounds quantified in the liquid tar sample from gasifier systems, which will exclude compounds evaporated during the determination of gravimetric tar. Thus, total tar refers to the sum of gravimetric tar and the tar in the evaporation residue [9].

Due to the complexity of tar, most reports are mainly concerned with the identification and quantification of PAH from pyrolysis or combustion. In the case of kinetic studies, attention has been given to the determination of either kinetic parameters for the overall weight loss of the fuel or kinetic parameters for the evolution of light gases (such as CO, CH_4 and H_2). As a result, kinetic data and theoretical comprehension of the tar reaction processes during bio-

mass gasification are still on-going research topics. Therefore, the present review evaluates the recent work on tar formation and evolution during fluidised bed biomass gasification. This work does not intend to be an exhaustive review of all the literature on lignocellulosic material and their tars; instead this work presents the fundamentals of tar formation, tar evolution and its destruction, which are applicable to models that include tar formation mechanisms.

2. Fundamentals of biomass tar formation

Biomass composition mainly comprises lignin, cellulose and hemicellulose. Table 1 shows the approximate analysis of some types of biomass [10–12]. During biomass pyrolysis, it has been identified that biomass decomposes according to the following four stages: at temperatures <493 K, moisture was evaporated; at 493–588 K, predominantly hemicellulose decomposition occurred; at 588–673 K, cellulose decomposition was observed; and at >673 K, mainly lignin decomposed [13]. However, differences in devolatilisation patterns, based on weight losses during thermogravimetric analysis (TGA) for different types of biomass, have been acknowledged. For example, TGA results for wood chips and chicken litter (broiler and flock) showed different weight loss regimes. Wood chips showed two weight loss regimes, the first one attributed to the decomposition of cellulose, hemicellulose and lignin, and the last one to the further devolatilisation of residual charcoal. Whereas chicken litter exhibited three different weight loss regimes, the second loss regime was attributed to manure and lignin, and the third one to further charcoal devolatilisation [14,15].

It is well established that gasification comprises sequential steps, which are: pre-heating and drying, pyrolysis, and char gasification and oxidation. The pyrolysis step normally takes place at 473–773 K, where the fuel decomposes into three often lumped products: char, volatiles (condensable hydrocarbon or tar) and gases (non-condensable) [16,17]. Since pyrolysis is the first stage of thermal degradation, the mechanisms of biomass pyrolysis have been studied to determine the pyrolysis rate and the amount, properties and composition of the resulting product [16,18].

Experiments using hinoki cypress sawdust were executed to compare pyrolysis, steam gasification and partial oxidation conditions [19]. It was found that pyrolysis (at 873 K) produced mainly oxygen-containing compounds, that is, primary tars, such as methanol, acetaldehyde, acetic acid, hydroxypropanone, methyl furfural, and cresols; and in minor quantities, aromatic compounds such as phenol, benzene and toluene. Higher temperatures (1173–1273 K) during pyrolysis and steam gasification produced less oxygen-containing compounds (only phenol and benzofuran), and mainly aromatic compounds (benzene and toluene) as well as of higher molecular weight, such as naphthalene, styrene, indene, anthracene, and pyrene. For steam gasification, even chrysene and benzopyrene were detected. In brief, secondary and tertiary tars were generated at those conditions. Lastly, pyrolysis and steam gasification at temperatures higher than 1373 K, and partial oxidation showed that most tar compounds were destroyed and only stable aromatics (benzene, toluene and naphthalene) remained. As a result, the study of pyrolysis reactions of tar precursors is also crucial for understanding tar decomposition during biomass gasification.

Table 1
Approximate analysis of some biomass types.

Type of biomass	Cellulose (%)	Hemicellulose (%)	Lignin (%)	Other (%)
Softwood[a]	41	24	28	7
Hardwood[a]	39	35	20	7
Wheat straw[a]	40	28	17	15
Rice straw[a]	30	25	12	33
Bagasse[a]	38	39	20	3
Oak wood[b]	34.5	18.6	28	
Pine wood[b]	42.1	17.7	25	
Birch wood[b]	35.7	25.1	19.3	
Spruce wood[b]	41.1	20.9	28	
Sunflower seed hull[b]	26.7	18.4	27	
Coconut shell[b]	24.2	24.7	34.9	
Almond shell[b]	24.7	27	27.2	
Broiler poultry litter[c]	27	17.8	11.3	20

[a] Other refers to organic compounds such as starch and inorganic material such as salts, minerals, and water [10].
[b] Lignin was measured as acid-insoluble lignin, %cellulose = %glucose × 0.9 and %hemicellulose = (%galactose + %mannose) × 0.9 + (%xylose + %arabinose) × 0.88 [11].
[c] Hemicellulose = NDF–ADF, and cellulose = ADF – lignin. NDF: neutral detergent fiber; ADF: acid detergent fiber. Other refers to crude ash [12].

2.1. Lignin

Lignin fraction normally consists of 20–40 wt.% dry of biomass. Lignin is a complex racemic polymer and is composed of p-hydroxyphenyl, guaiacyl and syringil units; an example of a typical lignin structure is shown in Fig. 1. Since only the lignin fraction of the biomass is aromatic in nature, lignin represents a potential precursor for PAH formation. Three hydroxycinnamyl alcohols considered precursors of lignin, which only differ in their degree of methoxylation, are shown in Fig. 2. The three species, p-coumaryl alcohol, coniferyl alcohol and sinapyl alcohol, are also called monolignols. These monolignols produce dilignols as the main building blocks of the lignin polymer, p-hydroxyphenyl, guaiacyl, and syringyl phenylpropanoid, respectively [20].

The lignin monomeric unit is often referred as nine carbon atoms and expressed using a C_9 based formula, e.g. $C_9H_{7.2}O_2(H_2O)_{0.4}(OCH_3)_{0.92}$ for Norway spruce. For spruce lignin a ratio of guaiacyl: p-hydroxyphenyl: syringyl units was estimated as 94:5:1 [21].

Lignin pyrolysis is known to produce non-condensable gases, char, and condensable tars comprising several low and high molecular weight phenolic compounds, at low to moderate temperatures (<973 K) [20]. Lignin was the most difficult to decompose among the three biomass components. Its decomposition occurred in a wide temperature range (373–1173 K), due to the broad range of activity of the chemical bonds in lignin aromatic rings [22]. Oxygenated compounds were the most dominant products during the pyrolysis of biomass from both cellulose and lignin; mainly guaiacols with some furans and sugar derivatives, such as levoglucosan, predominantly arose from cellulose even above 873 K [23].

2.1.1. Lignin pyrolysis products

Some typical products of lignin pyrolysis identified from experimental work are presented in Table 2 [24]. These pyrolysis products were mainly grouped in phenolics, such as phenols, guaiacols and catechols, and light gases e.g. carbon oxides. However, this list did not identify if the products were originally generated or evolved after reactions of previous products. To make a distinction, a mechanism that includes the reaction pathway from lignin precursors to larger PAHs is necessary.

Lignin from different types of biomass differs in structure, and expectedly in the primary pyrolysis products generated. Hardwood lignin comprises guaiacyl (4-hydroxy-3-methoxyphenyl) and syringyl (3,5-dimethoxy-4-hydroxyphenyl) units, while softwood lignin is mainly made of guaiacyl units. GC/MS studies showed that guaiacol (2-methoxyphenol) and syringol (2,6-dimethoxyphenol)

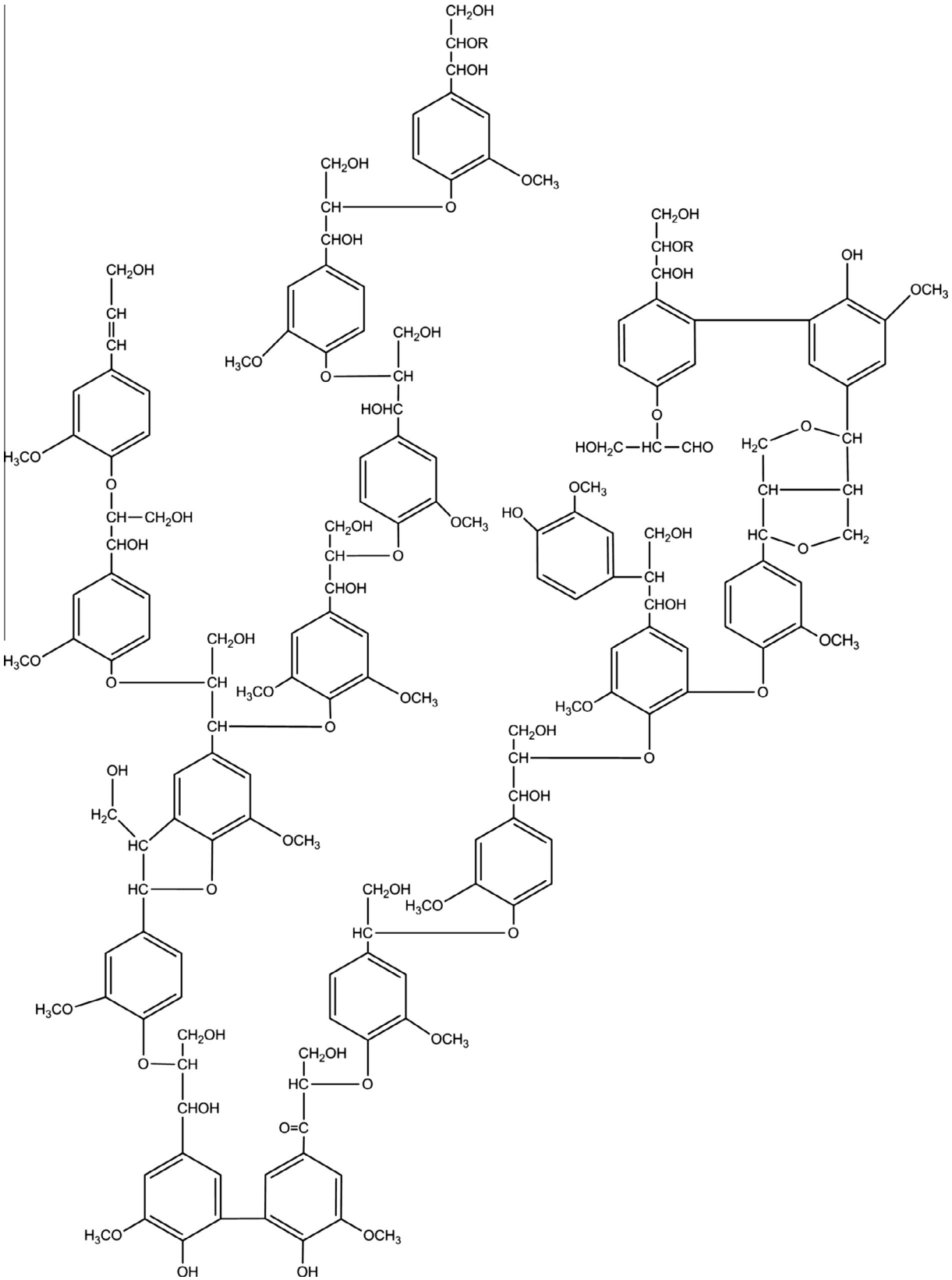

Fig. 1. Typical structure of a softwood lignin [20,21].

and their derivatives with various saturated, >C═C< and >C═O side-chains at their C4-positions were formed from hardwood lignin pyrolysis. Only guaiacol and its derivatives were produced from softwood lignins. Secondary reactions of these primary tars produced catechols/pyrogallols, cresols/xylenols, phenol, PAHs, coke and gases [25].

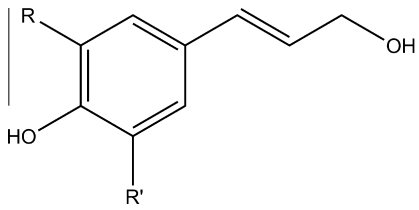

R,R' = H p-coumaryl alcohol
R = H, R' = OCH_3 coniferyl alcohol
R,R' = OCH_3 sinapyl alcohol

Fig. 2. Hydroxycinnamyl alcohols precursors of lignin.

Table 2
Typical lignin pyrolysis products [24].

Type of product	Group of compound	Examples
Light liquids	H_2O, metanol	
Phenolics	Monohydroxyl phenols	Phenol, o-cresol, m-cresol, p-cresol, 2-ethylphenol, 4-propylphenol and xylenols
	Guaiacols	Guaiacol, 4-methylguaiacol, 4-ethylguaiacol, 4-propylguaiacol
	Catechols	Catechol, 4-methylcatechol, 4-ethylcatechol, 3-methoxycatechol
Gases	Hydrocarbons	Methane, ethane, ethylene, propane, propylene, n-butane and isobutene
	Carbon oxides	CO, CO_2
	Sulphur-containing compounds	H_2S, methyl mercaptan

2.2. Cellulose

Cellulose has the empirical formula $H(C_6H_{10}O_5)_nOH$, where n is the number of monomer units, from 200 to ~10,000, with corresponding molecular weights of 32,400 to more than 1,600,000. Cellulose pyrolysis produced large amounts of carbohydrates, and levoglucosan was the main constituent of these carbohydrates [26]. TGA experiments have shown that cellulose primary pyrolysis took place at the temperature range of 600–680 K [27]. The maximum weight loss rate was reached at 628 K. When the temperature was higher than 673 K, nearly all cellulose was pyrolyzed and very low solid residue was left [22].

Experimental studies have shown that cellulose pyrolysis produced levoglucosan as an intermediate product, which then converted to tar compounds [28]. Besides levoglucosan, other primary tar components were produced after cellulose pyrolysis such as, furfural, glycolaldehyde, hydroxyacetone, formic acid and acetic acid. Increasing yields of CO, CH_4 and H_2 were linked to decreasing yields of levoglucosan, glycolaldehyde, formic acid and furfural [29].

2.2.1. Cellulose pyrolysis products

Cellulose pyrolysis has been reported to generate predominantly furans and small molecule aldehydes. The large number of furan-ring products was suggested as mainly caused by the competitive reactions of the formation of levoglucosan with the secondary decomposition of levoglucosan. The small molecule aldehydes were identified as mostly produced from the secondary decomposition of anhydrous sugars (especially levoglucosan) through dehydration, fission, decarbonylation and decarboxylation reactions [30].

"Broido-Shafizadeh" proposed a model for the pyrolysis of cellulose, which is one of the oldest and still widely acknowledged. This model showed the decomposition of cellulose as two consecutive first-order reactions. The first step generated an "active cellulose", followed by two competing reactions whereby it was either decomposed into char and gases (CO_2 and water vapor) or further depolymerised into volatiles with levoglucosan as its main constituent [10,31].

"Diebold" model consists of seven first-order global reactions for the pyrolysis of cellulose. First cellulose was decomposed through two competing reactions, one to produce "active cellulose" product, and the other a dehydration reaction to form char and water. The "active cellulose" material may be transformed in three ways in order to: crack directly to secondary gases; pyrolyze and volatilise to primary vapours; or dehydrate to char and water. The primary vapours could then react to form secondary gases or secondary tars (and by-product gases) [32].

Lin et al. [33] presented a mechanism in which cellulose decomposed to oligosaccharides with relatively lower molecular units up to it reached the sugar level resulting in levoglucosan production. Levoglucosan could undergo dehydration and isomerization reactions to form other anhydro-monosaccharides such as levoglucosenone, which could be either repolymerized or transformed by fragmentation to form aldehydes and ketones, dehydration to form furans, decarbonylation or decarboxylation.

In order to establish a pathway for cellulose pyrolysis, levoglucosan was chosen as a model compound since it was the main pyrolysis product formed. It was found that levoglucosan underwent two simultaneous reactions: transformation into volatile low-molecular weight products and ring-opening polymerisation into polysaccharides. The pyrolysis products were found to change stepwise as: levoglucosan → MeOH-soluble fraction (lower-molecular-weight products and oligosaccharides) → water-soluble fraction (polysaccharides) → insoluble fraction (carbonized products) [34].

2.3. Hemicellulose

Hemicellulose is a complex component of biomass, interconnected together with cellulose by physical intermixing, and linked to lignin by covalent bonds (mainly α-benzyl ether linkage). Hemicellulose is the least stable polymer within lignocellulosic biomass and is not chemically homogeneous [35]. In addition, hemicellulose is amorphous and has a lower degree of polymerisation than cellulose [36]. The main hemicellulose component is xylan, which is composed of 1,4-linked β-d-xylopyranose (β-d-Xyl*p*) units that can be substituted at C-2 and/or C-3 by short and flexible side chains. In addition, acetyl groups located at O-2 and/or O-3 are often found on the backbone of xylopyranosyl residues [35].

Hemicellulose is thermally the least stable component of biomass. For that reason, hemicellulose decomposed faster and at lower temperatures than cellulose and lignin [37]. Xylan started decomposing easily during pyrolysis, where the weight loss mainly happened at 493–588 K. The maximum mass loss rate occurred at 541 K, and ~20% solid residue was still left even at 1173 K [22].

2.3.1. Hemicellulose pyrolysis products

It has been reported that the main compounds from the pyrolysis of hemicellulose are methanol, acetic acid, furfural, acetone and 1,4-anhydro-D-xylopyranose. It was found that 1,4-anhydro-D-

xylopyranose acted as an intermediate product to generate two- and three-carbon fragments and gases. The main mechanism of the formation of acetic acid was suggested as involved with the primary elimination reaction of the active o-acetyl groups linked to the main xylan chain on C2 position; whilst the formation of acetic acid and CO_2 was attributed to the primary decomposition of the o-acetylxylan unit [38]. Table 3 shows the main hemicellulose monomeric units and their most important derived pyrolysis products.

It is known that xylan is the main hemicellulose component of hardwoods and glucomannans of softwoods [36]. Therefore, xylan has been used as a model compound of hemicellulose. From xylan pyrolysis, acids, phenols, aldehydes, ketones, and esters were detected and a small amount of carbohydrates. Xylan mainly formed acids which were derived from the acetyl groups and uronic acid side chains [26].

Xylan primary degradation was recognised from two overlapped steps represented by two peaks in the differential thermogravimetric (DTG) curves. The first peak was assigned to the cleavage of the glycosidic bonds between xylan units and the decomposition of side chain structures; the second peak was attributed to the opening of the xylan unit [27].

Pathways proposed for the pyrolytic gasification of different chemical structures of biomass components, cellulose and lignin are shown in Fig. 3 [29]. The experiments were carried out under the conditions of N_2 at 873 K without adding any gasifying agents in a closed ampoule reactor. It was found that the secondary char formation from wood polysaccharides (cellulose and hemicellulose) was caused by the condensation of volatile products such as levoglucosan. For lignin, the O—CH_3 homolysis was named responsible for the structural changes of the aromatic rings to form catechol-, o-cresol- and phenol-type compounds, and for the acceleration of the secondary char formation.

Table 3
Main hemicellulose pyrolysis products [38].

Monomeric unit	Functional group	Main compounds
Xylan	Alcohol	Ethanol
	Aldehydes	Acetaldehyde, propanedial, formaldehyde
	Heterocyclic aldehyde	Furfural
	Ketone	Acetone
	Gases	CO, CH_4, H_2
o-Acetyl xylan	Aldehydes	Acetaldehyde, formaldehyde
	Carboxylic acid	Acetic acid, propionic acid
	Ketone	Acetone
	Gases	CO_2, CO
4-o-Methyl glucurono-xylan	Alcohol	Methanol
	Aldehyde	Acetaldehyde, glycolaldehyde
	Carboxylic acid	Acetic acid, formic acid
	Heterocyclic aldehyde	Furfural
	Ketone	Acetone
	Gases	CO_2, CO

3. Methods of quantification

Biomass is composed largely of cellulose -a polymer of glucose-, hemicellulose -a complex polymer of which the main chain mostly consists of xylans-, and lignin -a complex phenolic polymer. Analytical methods have been developed over the years to estimate the composition of biomass components; these methods are mainly based on the fractionation of biomass samples, wherein the isolated and purified fractions are quantified using conventional analytical instruments [39].

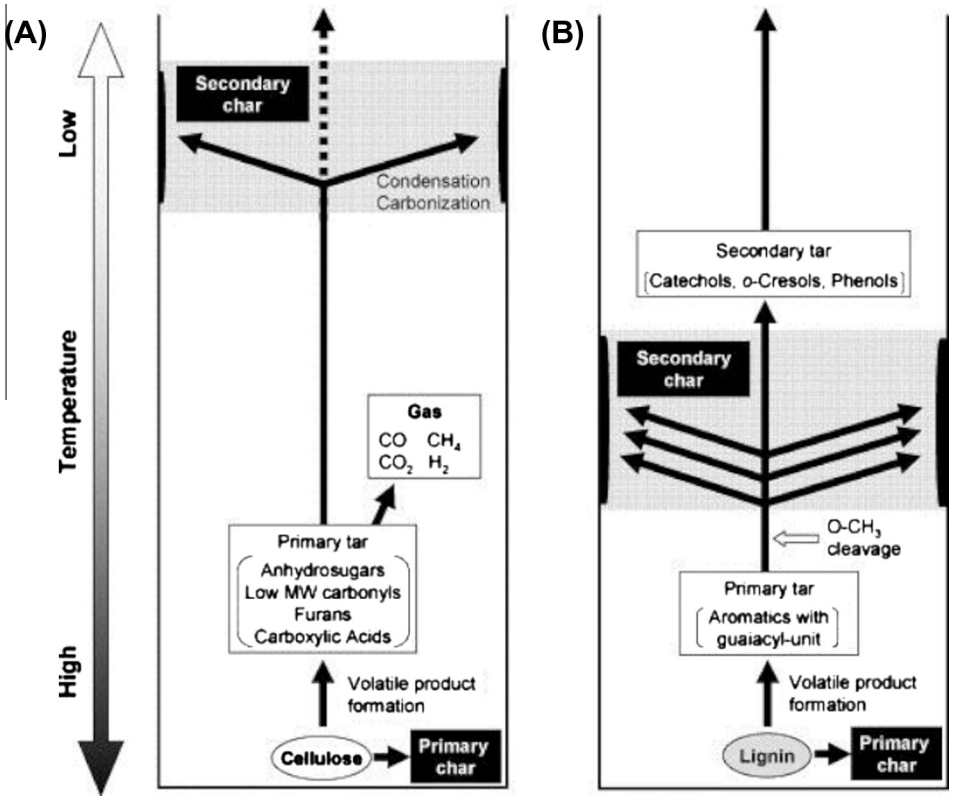

Fig. 3. Pyrolytic gasification pathways of cellulose (A) and lignin (B) [29].

3.1. Lignin quantification

The structure of lignin is complex and irregular, and additionally the preparation of pure samples of unchanged structure is not an easy task. There are two major groups of methods for lignin determination. The first group employs strong mineral acids, since lignin is mainly insoluble in mineral acids; lignin can be analysed gravimetrically after hydrolysing the cellulose and hemicellulose fractions with sulphuric acid. The second group uses oxidizing agents to selectively remove the lignin. In these second methods, lignin is estimated either by sample mass loss or through a photometric assay for lignin oxidation products [40].

The oldest and most common first-group method to determine the total lignin is the Klason lignin determination, which has been standardised by the Technical Association of the Pulp and Paper Industry. The sample is first treated with 72% sulphuric acid and then heated with dilute acid to hydrolyse the polysaccharides to soluble fragments. The solid residue is washed, dried and weighed. Correct values are obtained for softwoods, but hardwoods contain variable amounts of 'acid soluble lignin' which must be estimated by UV spectrophotometry [41]. The acid detergent lignin (ADL) method was developed by Van Soest (1967) and is a modification of the Klason lignin method. The main difference between the two methods is the sequence in which acid concentration and temperature are utilised to affect the hydrolysis of polysaccharides. In ADL analysis, dilute H_2SO_4 is used initially at high temperature, followed by more concentrated acid at low temperature [42]. The determination of the lignin content, as part of the biomass characterisation, is of particular interest as input parameter in modelling work.

3.2. Cellulose and hemicellulose quantification

Cellulose and hemicellulose fractions are insoluble in water. First, cellulose is solubilised by concentrated sulphuric acid, usually 72% (w/w) at 303 K, and then is hydrolysed by diluted H_2SO_4. Hemicellulose can be hydrolysed into their constituent monosaccharides by diluted H_2SO_4, usually 4% (w/w) at 394 K [43]. As a result, three methods are commonly employed for the determination of cellulose and hemicellulose – the acid detergent fibre (ADF), neutral detergent fibre (NDF) and ADL.

The NDF is the cell wall fraction which comprises cell wall polysaccharides (less pectins) and lignin. The NDF is obtained from an extraction with neutral detergent (sodium laurylsulphate) which removes cell contents and amorphous silica. The residue is directly filtered, washed with hot water, and dried with acetone. If followed by a calcination step at 823 K, the ash content can be determined [39]. The ADF, is the residue consisting of lignin and cellulose, obtained after extraction with acid detergent (acetyltrimethylammonium bromide in 0.5 M sulphuric acid at 373 K) and hydrolysis of the hemicellulose components [43]. Therefore, according to the Van Soest method, cellulose is determined by the difference between ADF and ADL and hemicellulose as NDF–ADF.

The holocellulose extraction (HOLO) procedure involves treatment with an acid solution (sodium acetate solution) at 348 K to brake off the non-covalent interactions between biomass polymers. Sodium chlorite is then added, followed by cooling, filtration and washing with water and acetone, in order to optimise the polymer hydrolysis whilst minimising the degradation of monomeric sugars. Lastly, the residue is dried at room temperature and weighted to measure the holocellulose content, which only contains cellulose and hemicellulose [39].

The α-cellulose (α) is termed as the residue of holocellulose insoluble in a NaOH solution (17.5 wt.%). It is considered to represent the undamaged higher molecular weight cellulose in biomass samples. Then, an acetic acid solution (10 wt.%) is added to hydrolyse the degraded cellulose and hemicelluloses. The residue is filtered and washed with hot water, and the α-cellulose is the dried residue, which is quantified gravimetrically [39].

4. Tar growth mechanisms

With the aim of understanding the generation of PAH leading to soot formation, some mechanisms are proposed in the literature as described below:

(i) Direct combination of aromatic rings, for example the combination of two rings to produce biphenyl as shown in Fig. 5.
(ii) H_2-abstraction-C_2H_2-addition (HACA) sequence. Aromatic rings grow by H-abstraction forming a radical compound, followed by acetylene addition which propagates molecular growth by cyclisation [44].
(iii) Phenol precursor for PAH formation. Phenol is transformed to cyclopentadiene and CO is abstracted from the phenol [45]. After that, cyclopendienyl radicals combine to form bigger compounds, e.g. aromatic compounds from naphthalene to chrysene, as shown in Fig. 6 [46].

Since the lignin fraction in biomass is relatively small, the HACA route to PAH formation was proposed as the more likely mechanism for soot formation [23]. Indeed, acetylene and butadiene were detected in significant concentrations during the combustion of pine wood [47]. Acetylene reached a maximum production between 1173 and 1273 K and complete destruction at 1473 and 1673 K for gasification and pyrolysis, respectively [19]. The decomposition of methoxyl groups and aliphatic chains were the main sources of light hydrocarbon gases. It was suggested that acetylene may derive from the decomposition of C_2H_4 and certain aromatic tar components. The yield of non-equilibrium intermediates (e.g. acetylene and ethylene) during pyrolysis was increased by high temperatures and short gas residence times [48].

Since acetylene reached maximum production and complete destruction at temperatures greater than 1173 and 1273 K for gasification and pyrolysis, respectively [19], the HACA route seems feasible only at temperatures greater than 1173 K, wherein acetylene is more abundant.

5. Tar destruction

Tar destruction takes place as a result of a series of complex, multiple and simultaneous reactions. The main reactions that might occur during tar decomposition were foreseen as:

Thermal cracking

$$pC_nH_x \leftrightarrow qC_mH_y + rH_2 \quad (1)$$

Steam reforming

$$C_nH_x + mH_2O \leftrightarrow nCO + \left(m + \frac{x}{2}\right)H_2 \quad (2)$$

Dry reforming

$$C_nH_x + nCO_2 \leftrightarrow 2nCO + \left(\frac{x}{2}\right)H_2 \quad (3)$$

Carbon formation

$$C_nH_x \leftrightarrow nC + \left(\frac{x}{2}\right)H_2 \quad (4)$$

Partial oxidation

$$C_nH_x + \frac{n}{2}O_2 \leftrightarrow nCO + \left(\frac{x}{2}\right)H_2 \quad (5)$$

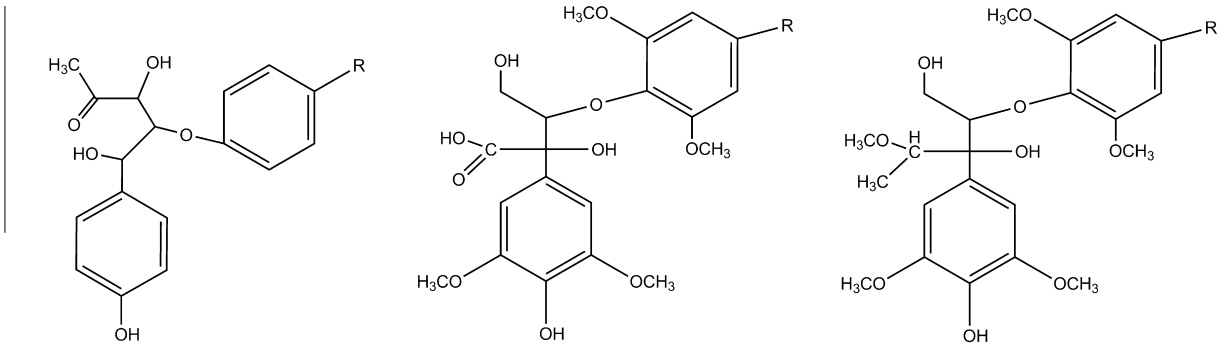

LIG-C $C_{17}H_{17}O_5$

67.8%C, 5.6%H, 26.6%O

LIG-O $C_{16}H_{11}O_6(OCH_3)_4$

56.7%C, 5.4%H, 37.8%O

LIG-H $C_{18}H_{17}O_5(OCH_3)_4$

60.4%C, 6.6%H, 33.0%O

Fig. 4. Model units in lignin structure [20].

where C_nH_x represented tar which can be a mixture of several individual tar compounds, and C_mH_y represented a hydrocarbon with a smaller carbon number than C_nH_x [49].

5.1. Tar model compounds

In order to overcome the complexity of the lignin structure, model compounds have been used as reference in experimental works for the characterisation of the different lignin units and identification of possible devolatilisation reactions. Some examples of model units are shown in Fig. 4. LIG-C represented a softwood lignin without methoxyl groups and with the largest amount of carbon [20]. LIG-O and LIG-H represented structures of hardwood lignin which are richest in O and H, respectively, containing methoxyl groups.

Eugenol (4-allyl-2-methoxyphenol, $C_{10}H_{12}O_2$) is other model compound that was used in order to represent the structural units of lignin. The major aromatic produced during pyrolysis was naphthalene, with methylnaphthalenes and other 2- and 3-ring PAHs [23]; during combustion mainly monoaromatics such as benzene, toluene and C_2-benzenes, were generated [47].

Catechol (1,2-dihydroxybenzene) has been used because it is a predominant unit in lignin and coal, as well as present in biomass tars [50]. Catechol was pyrolysed in the presence of various amounts of oxygen. Two-ring compounds, mainly indene and naphthalene were detected under pyrolysis or oxygen-rich conditions below 1073 K; whilst in the absence of oxygen, larger PAHs were produced and decreased with increasing oxygen content above 1073 K [47]. Experiments using a residence time of 0.4 s in a reactor operated at 773–1273 K showed that benzene was the most abundant aromatic produced during catechol pyrolysis (maximum yield 6.7% w/w at 1173 K), followed by naphthalene and indene [50].

The thermal cracking of methoxyphenols (ortho-, meta-, and para-guaiacol) were studied in a heated microtubular reactor. It was found that the three guaiacols decomposed to CH_3 and the hydroxyphenoxy radical, o-HO—C_6H_4O. Phenoxy radicals decarbonylated and the loss of CO generated the hydroxycyclopentadienyl radical, which further decomposed to phenol [51].

Acetylene, C_2H_2, was found as an abundant product from pyrolysis during experiments using catechol as a model compound of lignin. It was proposed to add to benzene or phenyl radicals for producing styrene and phenylacetylene, or add to naphthalene, phenanthrene and pyrene for the formation of cyclopenta-fused PAHs [50].

5.2. Catalytic tar destruction

Due to the complexity of tar, its decomposition reactions have been studied using tar model compounds, such as phenol, toluene, naphthalene, etc. The catalytic activity of olivine via steam reforming was investigated using naphthalene as tar model. Naphthalene conversion was higher than 80% when pre-treated olivine (10 h of pre-treatment with air at 1173 K) was employed. The Arrhenius' law was applied to estimate the apparent activation energy over pre-treated olivine as 187 kJ/mol and frequency factor of 2.06×10^9 $m^3/kg\ h$ [52].

Toluene was used as tar model component in a laboratory scale fixed bed reactor for toluene steam-reforming. The highest conversion of toluene was achieved at temperatures above 923 K. The toluene conversion using a Ni/olivine catalyst at 833 K was the same as with olivine at 1123 K. The first order kinetic parameters for toluene steam-reforming on Ni/olivine were reported for the activation energy (E_A) as 196 kJ/mol and frequency factor (A) as 3.14×10^{13} $m^3/(kg_{cat}\ h)$ [53]. Benzene was also used as model component for kinetic studies at 1023–1198 K and ambient pressure in a fixed bed reactor with a mixture of simulated gasification gases using calcined dolomite as catalyst. The main assumed reactions were benzene reacting with water to produce CO, H_2 and CO_2, and benzene reacting with H_2 to form light hydrocarbons [54].

Experimental studies on fluidised bed gasification of pine sawdust included the application of calcined dolomite as catalyst, and air and steam as gasifying agents. After the gasifier, a fixed bed reactor with nickel based catalyst (Z409R) was incorporated for catalytic tar reduction. The temperature of the fixed bed reactor was varied by external heating and an optimal temperature of 1023 K to deliver the maximum H_2/CO ratio was found. Tar was reduced in the presence of the nickel based catalyst and also by

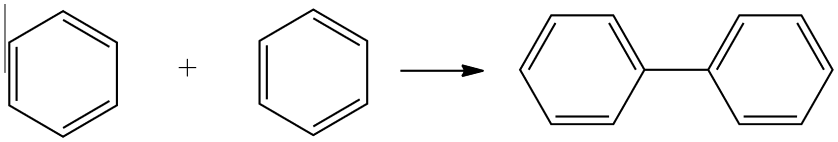

Fig. 5. Example of direct combination of aromatic rings.

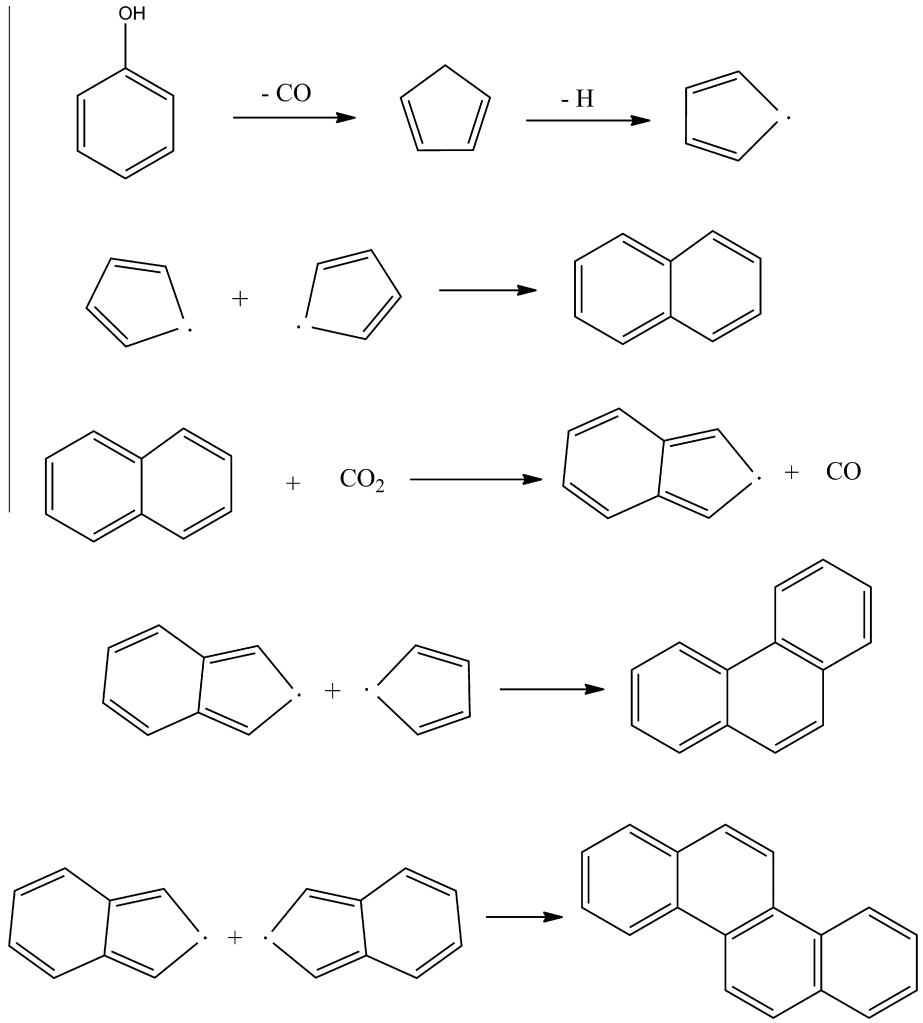

Fig. 6. PAH formation from phenol precursors [46].

increasing the temperature. Assuming a first-order kinetic model, all tar species were treated as one lump in order to avoid the complexity of the tar composition. E_A and A were determined as 51 kJ/mol and 14,476 $m^3(T_{b,wet})$/kg h, respectively [55]. Table 4 shows a summary of the kinetics obtained for tar model compounds and real tars during catalytic treatment. The apparent frequency factor ($k_{0,app}$) and activation energies (E_{app}) were provided based on the Arrhenius equation:

$$k_{app} = k_{0,app} e^{\left(-E_{app}/RT\right)} \quad (6)$$

Char has also been employed for the catalytic cracking of tars. Experiments for comparing different catalysts revealed that commercial biomass char delivered moderate phenol conversion (82% by mass) at 973 K; the ranking of catalysts activity observed for phenol conversion was: nickel > dolomite > fluid catalytic cracking > commercial biomass char > olivine > sand; whilst for naphthalene conversion at 1173 K: nickel > commercial biomass char > biomass char > biomass ash > fluid catalytic cracking > dolomite > olivine > silica sand [56]. In contract, experiments using pyrolysis vapours from wood passed through a hot char bed, reported no significant increase in the cracking of the tar yield [57]. The differences between the two above-mentioned experiments were the size of char particles and activation of char. Particles and void fraction in Abu El-Rub et al.'s [56] study (particle size of 1.4–1.7 mm with bulk density of 260 kg/m^3) were smaller than in the Gilbert et al.'s [57] study (char cubes of about 10 mm in size with bulk density of 100 kg/m^3), which increased the specific interfacial surface area for the tar compounds to be decomposed. In addition, the char in Abu El-Rub et al.'s [56] study was continuously activated by injecting steam (10%) and CO_2 (6%), which helped removing the coke deposits forming from the tar conversion on the char surface; whilst the Gilbert et al.'s [57] study used pure nitrogen as purge gas.

The benefits of char as a catalyst are its low cost and its natural production inside the gasifier. However, its disadvantages are coke formation which can block the pores of char and reduce the surface area of the catalyst, and catalyst loss due to char gasification by steam and dry reforming reactions [4].

5.3. Thermal tar destruction

Thermal tar destruction takes place at high operating temperatures wherein the total number of detectable tars was reduced; nonetheless, the formation of aromatics without substituent groups (such as benzene and naphthalene) was favoured [5]. In addition, increases in the freeboard temperature also contributed to the reduction of tar content due to tar cracking and steam reforming reactions [68]. Table 4 shows the kinetic parameters for some tar model compounds obtained during thermal treatment.

Tar conversion processes have been simulated using numerical methods in order to understand the cracking of tar as a secondary

Table 4
Kinetic parameters for the decomposition of some tar model compounds and real tars: thermal and catalytic cracking.

Model tar	Agent	Catalyst bed		Kinetic parameters		Ref.
		Type	Temperature (K)	E_{app} (kJ mol^{-1})	$k_{0,app}$ ($m^3_{T,wet}$ kg^{-1} h^{-1})	
Thermal cracking						
Benzene[a]	$H_2O + H_2$		1073–1673	443	2×10^{16}	[58]
Toluene[b]	$H_2O + H_2$		973–1673	247	3.3×10^{10}	[58]
Toluene	$H_2O + O_2$		973–1223	356	2.3×10^5 s^{-1}	[59]
Toluene[c]	$N_2 + H_2 + H_2O$		1098–1223	250	3.3×10^{10}	[59]
Naphthalene[d]	$H_2O + H_2$		1223–1673	350	1.7×10^{14}	[58]
Catalytic cracking						
Naphthalene	$H_2O + CO_2 + CO + H_2$	Pretreated olivine	1098–1173	187	2.06×10^9	[52]
Naphthalene	Air	Pt/Al_2O_3	726–753	149.9	3.26×10^{17}	[60]
Naphthalene	$H_2O + CO_2$	Char	973–1173	61	7.6×10^4	[56]
Naphthalene	H_2	Ni–Fe-dolomite	923–1223	63.9		[61]
1-methyl-naphthalene	$N_2 + H_2$	NiMo	823	66.6	3.12×10^{-4} s^{-1}	[62]
		Y-zeolite		37.2	5.68×10^{-5} s^{-1}	
Toluene	H_2O	Ni/olivine	833–1123	196	3.14×10^{13}	[53]
Tar from biomass gasification	Air	Dolomite/sand	1123	196	7.2×10^{10}	[63]
		Olivine/sand		114	3.6×10^6	
Tar from Mallee wood pyrolysis	H_2O	Char	773–1123	82.1	5.39×10^6	[64]
		Char/iron		60.8	2.11×10^6	
		Char/nickel		57.3	1.32×10^6	
Tar from biomass gasification	H_2O	BASF G1-50	1003–1123	40	23,460	[65]
		ICI 46-1		40	23,100	
Tar from biomass gasification	Air	Calcined dolomites	1053–1193	100 ± 20	$1.2–1.5 \times 10^6$	[66]
Tar from pine sawdust gasification	Air + H_2O	Nickel based of Z409R	923–1123	51	14,476	[67]

[a] Units for $k_{0,app}$ mol 0.1 m$^{-0.3}$ s^{-1}. Reaction order with respect to naphthalene 1.3, H_2 −0.4 and H_2O 0.2.
[b] Units for $k_{0,app}$ m$^{1.5}$ mol s^{-1}. Reaction order with respect to naphthalene 1, and H_2 0.5.
[c] Units for $k_{0,app}$ m$^{1.5}$ mol s^{-1}.
[d] Units for $k_{0,app}$ m$^{1.5}$ mol$^{-0.5}$ s^{-1}. Reaction order with respect toluene 1, and gas mixture 0.5.

method inside a second reactor. Thermal degradation of tar in a secondary gasification unit called Turboplasma® was modelled using a kinetic model, where the plasma gas was air heated to temperatures up to 5000 K close to the torch. Tar was represented by naphthalene and toluene, and a reaction pathway and its associated kinetics were provided. A total of eleven species were involved in 15 reactions using a completely stirred tank reactor (CSTR) model in order to only analyse the performance of the kinetic model. This pathway was based on the thermal cracking of tar into soot and hydrogen, and on the reforming of naphthalene and toluene into benzene and methane by water [69].

Other model used benzene, phenol, toluene and naphthalene as tar model compounds to simulate the tar destruction under partial oxidation conditions. Primary tars were produced in a pyrolysis unit, and then sent to a tube reactor for tar decomposition by partial oxidation. Fluid flow (k–ε turbulence model), kinetics of homogeneous reactions and heat transfer (Discrete Ordinates model) were included in the model. Steam reforming reactions were proposed for toluene and phenol. Hydrocarbons were converted to CO and H_2O by oxidation. Naphthalene was also formed from phenol pyrolysis and naphthalene reactions produced soot, benzene, CH_4 and H_2 [70]. A qualitative agreement was simply reported between the predicted tar amounts and those measured experimentally.

6. Methods for tar modelling

Based on the literature available, existing methods for the modelling of tar can be divided in single compound models, lumped models and detailed kinetic models, which will be described in more detail below.

6.1. Single compound models

Due to the identification of tar compounds from experimental work, the most frequent individual tar species studied experimentally and as tar model compounds are: acetol, acetic acid and guaiacols (primary tars); phenols, cresols and toluene (secondary tars); and naphthalene (tertiary tar).

Naphthalene was studied under pyrolysis conditions in a hydrogen and steam environment. The main products from naphthalene cracking were benzene, methane and C_2 hydrocarbons (mainly ethane); whilst minor products were indene, dihydro-naphthalene and toluene. Soot was produced, and at temperatures higher than 1373 K, CO and CO_2 originated from further cracking of soot and hydrocarbons [58].

Toluene was chosen as tar model because it is a stable aromatic compound formed during pyrolysis. A thermodynamic model was developed for biomass pyrolysis, and constrains on carbon were imposed for allowing toluene to produce other thermodynamically unstable hydrocarbons, such benzene, styrene, phenol and naphthalene. However, benzene and naphthalene were the only aromatic hydrocarbons produced [71].

Phenol was used as tar model compound for air-blown biomass fluidised bed gasification since phenol is known as a primary pyrolysis product [72]. Phenol cracking reactions involved the generation of naphthalene and benzene, as well as the decomposition of phenol, naphthalene and benzene to non-condensable gases and water.

Additionally, naphthalene formation was proposed from a series of two reactions [9]; first gravimetric tar was converted to intermediate compounds such as phenols ($A = 1 \times 10^4$ s^{-1}, and $E_A = 136$ kJ mol^{-1}), then naphthalene was formed ($A = 1 \times 10^7$ s^{-1}, and $E_A = 100$ kJ/mol). More tar model compounds were already discussed in Sections 5.1 and 5.2. Table 4 shows some tar model compounds that have been used to better understand tar destruction.

6.2. Lumped models

In order to simplify the simulation of a bubbling fluidised bed gasifier, tar conversion has been modelled assuming that all tar compounds constitute a single lump. For miscanthus and wood pellets gasification, the kinetic parameters derived from TG-FTIR

analyses were used for the flash pyrolysis step, which included the tar production; then, tar underwent a single decomposition step, according to the following reaction: $C_xH_yO_z \rightarrow zCO + \frac{1}{4}yCH_4 + (x - y - \frac{1}{4}y)C$, where $C_xH_yO_z$ represented tar [73]. The model and experimental data showed better agreement for NH_3 and light hydrocarbons than for H_2, CO and CO_2. The variations were attributed to unknown pyrolysis yields for H_2 and the use of a simple tar-cracking model.

Biomass gasification has been modelled assuming the primary pyrolysis of biomass as a first reaction, which produced CO, CO_2, H_2, CH_4, H_2O, N_2 and tar. In order to balance the equation, the tar formula was established as $CH_{1.522}O_{0.0228}$, which then experienced further secondary pyrolysis or tar cracking, and tar combustion according to [74]:

$$CH_{1.522}O_{0.0228} + 0.867O_2 \rightarrow CO + 0.761H_2O \quad (7)$$

Similarly, a generalised biomass gasification reaction was presented to account for the tar formation as followed:

$$CH_xO_yNz + wH_2O + m(O_2 + 3.76N_2) \rightarrow n_{H2}CO + n_{CO}CO_2 + n_{H2}H_2 + n_{CH4}CH_4 + n_{H_2O}H_2O + (z/2 + 3.76m)N_2 + n_{tar}CH_pO_q \quad (8)$$

where CH_pO_q was represented by the formula $CH_{1.003}O_{0.33}$, and as input parameter the maximum tar yield of 4.5% (mass percentage) was fixed on the model based on previous experimental tar measurements [75].

Since most works have grouped all tar compounds as a single unit, an improved kinetic model was developed to treat tar as composed of six lumps. Each lump consisted of tar species with similar chemical structure. The six lumps considered were: (i) benzene, (ii) one-ring compounds (except benzene), (iii) naphthalene, (iv) two-ring compounds (except naphthalene), (v) three- and four-ring compounds, and (vi) phenolic compounds [76]. Based on the experimental work on the evolution of tar composition, a set of six kinetic equations with eleven different kinetic constants was presented. Reactivity rates were evaluated and it was found that phenolic compounds were the most reactive (296 mg destroyed/kg of catalyst/h), and naphthalene was the hardest compound to be destroyed (33.1 mg destroyed/kg of catalyst/h). The kinetic equations fitted well with the experimental results. Nevertheless, the experimental data were obtained using the solid-phase adsorption method for tar sampling. Heavy tars (compounds with high molecular weight) are not trapped by this sampling method; therefore, the developed kinetic model has the same limitations. This shows that care should be taken when using tar models which employed experimental data with selected tar compounds. Especially when heavy tar compounds are neglected since these compounds might condense even at high temperatures and low concentrations.

For the modelling of high temperature steam gasification of woody biomass, the tar composition was calculated as a mixture of acetol, toluene and naphthalene [77]. The pyrolysis reaction was described as:

$$\text{Biomass} \rightarrow a_1\text{Char} + a_2\text{Tar} + a_3H_2 + a_4CO + a_5CO_2 + a_6CH_4 + a_7C_2H_4 \quad (9)$$

The pyrolysis product yields were taken from experimental pyrolysis work, up to a temperature of 1173 K. Eleven reactions, which included the evolution of the three tar compounds, were considered. It was found that tar concentration from steam gasification was higher than from air or oxygen-blown gasification [77,78]. The numerical analysis over predicted CH_4 and under predicted H_2.

A model for biomass gasification in a dual fluidized bed (DFB) reactor was presented [79]. Correlations determined from experiments and detailed tar analyses at reactor temperatures between 973 and 1273 K and for average particles heating rates between 293 and 313 K/s were used. The correlations provided the mass yields of pyrolysis products, including main permanent gases (CO, H_2, CO_2, CH_4, C_2H_4, and C_2H_6), water, and ten tars species. In order to simplify the model, the ten tars species were grouped into four lumps: (a) benzene (benzene), (b) phenol (phenol and cresols), (c) toluene (toluene, o-xylene and indene), and (d) naphthalene (naphthalene, 1 + 2methylnaphthalene, acenaphthylene and phenanthrene). The simulation results were in good agreement with experiments since the pyrolysis correlations were obtained from the same experimental test facilities.

6.3. Detailed kinetic models

Detailed kinetic models have been developed, which involve reaction mechanisms comprising hundreds of elementary step-like reactions, in order to provide a more accurate description of the gas-phase reactions concerning aromatic growth [80].

With the aim of predicting lignin devolatilisation from TGA pyrolysis experiments, a "semi-detailed" kinetic mechanism was proposed. The model used three reference lignin units to represent the initial lignin structure, 100 molecular and radical species were involved in the mechanism, and the mass balances included the net rate of formation. Experimental TGA literature data from a variety of pyrolysed lignins were compared to the model predictions [20]. The model results agreed with the experimental thermal degradation of lignins, only the total mass loss at low pyrolysis temperatures was underestimated at isothermal devolatilisation.

A semi-detailed chemical reaction mechanism for toluene reference fuels was developed, which incorporated 137 species and 633 reactions. The model included a detailed reaction mechanism for toluene and mechanisms for the combustion of the primary reference fuels: iso-octane (2,2,4-trimethylpentane) and *n*-heptane [81]. One initiation reaction was the oxidation of toluene to produce benzyl ion. The aim for this model was to evaluate if using mixtures of toluene with primary reference fuels could emulate real gasoline. The model was compared against shock tube ignition delay experimental data for toluene and real gasoline; it was shown better prediction of the temperature dependence at the leanest fuel–air ratio of 0.25, and in perfectly stirred reactor conditions.

A detailed chemical kinetic model, to simulate the gas-phase reactions in chemical vapour deposition of carbon from ethylene, acetylene, and propylene, was developed [82]. The gas-phase reaction mechanism involved 227 species and 827 elementary reactions, 798 of which were reversible. Experimental data from a conventional flow reactor were used to validate the model. Acetylene was assumed to be firstly consumed by dimerization to form vinylacetylene, and secondly by diacetylene formation. Combination of acetylene and vinylacetylene contributed to the acetylene consumption and benzene formation. PAH formation was underpredicted, and the deviations were mostly greater as the molecular size of the PAH increased. An improved version for the pyrolysis of ethylene, acetylene, and propylene was presented, and the detailed kinetic model comprised the formation of PAHs up to coronene [80]. The upgraded mechanism consisted of 241 species and 902 elementary step-like reactions. For acetylene pyrolysis, acetylene was proposed to react with methyl radical to form 2-methylvinyl radical, which converted into allyl radical by isomerization. The best improvement in this model was the addition of reactions among cyclopentadienyl, indenyl, and benz[f]indenyl radicals to form benz[a]anthracene and chrysene.

The steam reforming of aromatic hydrocarbons was modelled using a detailed chemical kinetic model [83]. The model results were validated with previous experimental data from the thermal

conversion of naphthalene, benzene, and toluene [58]. The reaction mechanism comprised 257 chemical species, from hydrogen radicals to coronene, and 2216 reactions. Comparisons of the experimental data with the model showed good agreement, especially for the conversion trends of the three aromatic hydrocarbons and the yield of major products, such as methane and benzene. However, soot was under predicted and C_2 hydrocarbons overpredicted. There were two major proposed pathways for the conversion of naphthalene. The first was the decomposition into smaller species, from naphthalene reaction with OH radical to form napththol, through indenyl and indene formation, up to vinylacetylene, toluene and benzene formation. The second was the combination of naphthalene and naphthyl radical to form perylene, which further grew into coronene in a step-wise mode via benzo[ghi]perylene through the HACA mechanism.

A detailed chemical kinetic model was applied for the gas-phase reactions involved in the secondary pyrolysis of cellulose; the elementary reactions were compiled and then estimated using the automatic reaction generating software (RMG) [84]. The kinetic model comprised more than 500 species and more than 8000 reactions. The numerical results were compared with data from a two-stage tubular reactor used for cellulose pyrolysis. Both approaches agreed in the prediction of inorganic gases, acetylene and acetic acid; however, the trends for propylene and propane were incorrectly predicted at 973 K. Agreement regarding minor products such as acetaldehyde, acetone, hydroxyl acetone, furan, benzene, and toluene were fair; whilst predictions for methanol and C_3 hydrocarbons needed improvement. The possible reaction pathways leading to benzene were identified. Two dominating routes were suggested: the first was the decomposition of toluene, and the second was from C_3 hydrocarbons such as propadiene and propyne.

In summary, tars are normally modelled as a "lump" or by using the most stable components such as toluene, benzene and naphthalene; however, these species are known to appear as secondary and/or tertiary tars and the mechanisms and kinetics of their formation are often omitted. On the other hand, a detailed kinetic model that includes hundreds of species becomes a complex problem when being incorporated to simulate the conversion of biomass inside the gasifier. Therefore, a mechanism that could describe the formation of tars while maintaining a minimum number of tar species represents a more practical solution for tar simulation during biomass gasification.

7. Conclusions

A review of the background on tar evolution, main tar precursors and models that simulate tar formation and evolution was presented. A classification of tar compounds based on the evolution of tar according to temperature increments divides them into primary, secondary and tertiary tars. The most frequent individual tar species studied experimentally and as model tars are acetol, acetic acid and guaiacols (primary tars), phenols, cresols and toluene (secondary tars), and naphthalene (tertiary tar). Tars are typically modelled as a "lump" or using the most stable components; however, these species mostly appear as secondary and/or tertiary tars and their mechanisms and kinetics of formation are often ignored. A compromise between a kinetic model, that contains as much tar species as possible to represent lignin devolatilisation, and a mechanism, that could describe the formation of tars with minimum reactions, seems a better solution for tar simulation during biomass gasification. Among the mechanisms found for the PAH growth, the HACA route only is feasible at temperatures greater than 1173 K, wherein acetylene is more abundant. This review is taken as the framework to propose a mechanism for tar formation and evolution, which is then incorporated in a kinetic model of a fluidised bed gasifier [85].

References

[1] McKendry P. Energy production from biomass (part 1): overview of biomass. Bioresour Technol 2002;83:37–46.
[2] Devi L, Ptasinski KJ, Janssen FJJG. A review of the primary measures for tar elimination in biomass gasification processes. Biomass Bioenerg 2003;24:125–40.
[3] Han J, Kim H. The reduction and control technology of tar during biomass gasification/pyrolysis: an overview. Renew Sust Energ Rev 2008;12:397–416.
[4] Anis S, Zainal ZA. Tar reduction in biomass producer gas via mechanical, catalytic and thermal methods: a review. Renew Sust Energ Rev 2011;15:2355–77.
[5] Kinoshita CM, Wang Y, Zhou J. Tar formation under different biomass gasification conditions. J Anal Appl Pyrol 1994;29:169–81.
[6] Knight RA. Experience with raw gas analysis from pressurized gasification of biomass. Biomass Bioenerg 2000;18:67–77.
[7] Fagbemi L, Khezami L, Capart R. Pyrolysis products from different biomasses: application to the thermal cracking of tar. Appl Energy 2001;69:293–306.
[8] Nair SA, Yan K, Pemen AJM, Winands GJJ, van Gompel FM, van Leuken HEM, et al. A high-temperature pulsed corona plasma system for fuel gas cleaning. J Electrostat 2004;61:117–27.
[9] Morf P, Hasler P, Nussbaumer T. Mechanisms and kinetics of homogeneous secondary reactions of tar from continuous pyrolysis of wood chips. Fuel 2002;81:843–53.
[10] Shafizadeh F. Introduction to pyrolysis of biomass. J Anal Appl Pyrol 1982;3:283–305.
[11] Antal MJ, Allen SG, Dai X, Shimizu B, Tam MS, Grønli M. Attainment of the theoretical yield of carbon from biomass. Ind Eng Chem Res 2000;39:4024–31.
[12] Kwak WS, Jung SH, Kim YI. Broiler litter supplementation improves storage and feed-nutritional value of sawdust-based spent mushroom substrate. Bioresour Technol 2008;99:2947–55.
[13] Yang H, Yan R, Chen H, Zheng C, Lee DH, Liang DT. In-depth investigation of biomass pyrolysis based on three major components: hemicellulose, cellulose and lignin. Energy Fuels 2006;20:388–93.
[14] Kim S-S, Agblevor FA. Pyrolysis characteristics and kinetics of chicken litter. Waste Manage 2007;27:135–40.
[15] Font-Palma C. Characterisation, kinetics and modelling of gasification of poultry manure and litter: an overview. Energ Convers Manage 2012;53:92–8.
[16] Di Blasi C. Modeling chemical and physical processes of wood and biomass pyrolysis. Prog Energ Combust Sci 2008;34:47–90.
[17] Basu P, Kaushal P. Modeling of pyrolysis and gasification of biomass in fluidized beds: a review. Chem Prod Process Model 2009:4 [Article 21].
[18] Rapagnà S, Mazziotti di Celso G. Devolatilization of wood particles in a hot fluidized bed: Product yields and conversion rates. Biomass Bioenerg 2008;32:1123–9.
[19] Zhang Y, Kajitani S, Ashizawa M, Oki Y. Tar destruction and coke formation during rapid pyrolysis and gasification of biomass in a drop-tube furnace. Fuel 2010;89:302–9.
[20] Faravelli T, Frassoldati A, Migliavacca G, Ranzi E. Detailed kinetic modeling of the thermal degradation of lignins. Biomass Bioenerg 2010;34:290–301.
[21] Adler E. Lignin chemistry—past, present and future. Wood Sci Technol 1977;11:169–218.
[22] Yang H, Yan R, Chen H, Lee DH, Zheng C. Characteristics of hemicellulose, cellulose and lignin pyrolysis. Fuel 2007;86:1781–8.
[23] Fitzpatrick EM, Bartle KD, Kubacki ML, Jones JM, Pourkashanian M, Ross AB, et al. The mechanism of the formation of soot and other pollutants during the co-firing of coal and pine wood in a fixed bed combustor. Fuel 2009;88:2409–17.
[24] Jegers HE, Klein MT. Primary and secondary lignin pyrolysis reaction pathways. Ind Eng Chem Proc Des Dev 1985;24:173–83.
[25] Asmadi M, Kawamoto H, Saka S. Gas- and solid/liquid-phase reactions during pyrolysis of softwood and hardwood lignins. J Anal Appl Pyrol 2011;92:417–25.
[26] Qu TT, Guo WJ, Shen LH, Xiao J, Zhao K. Experimental study of biomass pyrolysis based on three major components: hemicellulose, cellulose, and lignin. Ind Eng Chem Res 2011;50:10424–33.
[27] Giudicianni P, Cardone G, Ragucci R. Cellulose, hemicellulose and lignin slow steam pyrolysis: thermal decomposition of biomass components mixtures. J Anal Appl Pyrol 2013;100:213–22.
[28] Nishimura M, Iwasaki S, Horio M. The role of potassium carbonate on cellulose pyrolysis. J Taiwan Inst Chem E 2009;40:630–7.
[29] Hosoya T, Kawamoto H, Saka S. Pyrolysis gasification reactivities of primary tar and char fractions from cellulose and lignin as studied with a closed ampoule reactor. J Anal Appl Pyrol 2008;83:71–7.
[30] Lv G, Wu S. Analytical pyrolysis studies of corn stalk and its three main components by TG-MS and Py-GC/MS. J Anal Appl Pyrol 2012;97:11–8.
[31] Ronsse F, Bai X, Prins W, Brown RC. Secondary reactions of levoglucosan and char in the fast pyrolysis of cellulose. Environ Prog Sust Energy 2012;31:256–60.
[32] Diebold JP. A unified, global model for the pyrolysis of cellulose. Biomass Bioenerg 1994;7:75–85.

[33] Lin Y-C, Cho J, Tompsett GA, Westmoreland PR, Huber GW. Kinetics and mechanism of cellulose pyrolysis. J Phys Chem C 2009;113:20097–107.
[34] Kawamoto H, Murayama M, Saka S. Pyrolysis behavior of levoglucosan as an intermediate in cellulose pyrolysis: polymerization into polysaccharide as a key reaction to carbonized product formation. J Wood Sci 2003;49:469–73.
[35] Sun Y-C, Wen J-L, Xu F, Sun R-C. Structural and thermal characterization of hemicelluloses isolated by organic solvents and alkaline solutions from Tamarix austromongolica. Bioresour Technol 2011;102:5947–51.
[36] Sullivan AL, Ball R. Thermal decomposition and combustion chemistry of cellulosic biomass. Atmos Environ 2012;47:133–41.
[37] Burhenne L, Messmer J, Aicher T, Laborie M-P. The effect of the biomass components lignin, cellulose and hemicellulose on TGA and fixed bed pyrolysis. J Anal Appl Pyrolysis 2013;101:177–84.
[38] Shen DK, Gu S, Bridgwater AV. Study on the pyrolytic behaviour of xylan-based hemicellulose using TG–FTIR and Py–GC–FTIR. J Anal Appl Pyrol 2010;87:199–206.
[39] Carrier M, Loppinet-Serani A, Denux D, Lasnier J-M, Ham-Pichavant F, Cansell F, et al. Thermogravimetric analysis as a new method to determine the lignocellulosic composition of biomass. Biomass Bioenerg 2011;35:298–307.
[40] Jung HG, Mertens DR, Payne AJ. Correlation of acid detergent lignin and Klason lignin with digestibility of forage dry matter and neutral detergent fiber. J Dairy Sci 1997;80:1622–8.
[41] Brunow G. Methods to reveal the structure of lignin. In: Hofrichter M, Steinbüchel A, editors. Biopolymers: Wiley-VCH; 2001.
[42] Hatfield RD, Jung H-JG, Ralph J, Buxton DR, Weimer PJ. A comparison of the insoluble residues produced by the Klason lignin and acid detergent lignin procedures. J Sci Food Agric 1994;65:51–8.
[43] Lowry JB, Conlan LL, Schlink AC, McSweeney CS. Acid detergent dispersible lignin in tropical grasses. J Sci Food Agric 1994;65:41–9.
[44] Frenklach M, Wang H. Detailed mechanism and modeling of soot particle formation. In: Bockhorn H, editor. Soot formation in combustion: Mechanisms and Models: Springer-Verlag; 1994. p. 165–90.
[45] Cypres R, Bettens B. Mecanismes de fragmentation pyrolytique du phenol et des cresols. Tetrahedron 1974;30:1253–60.
[46] Sharma RK, Hajaligol MR. Effect of pyrolysis conditions on the formation of polycyclic aromatic hydrocarbons (PAHs) from polyphenolic compounds. J Anal Appl Pyrol 2003;66:123–44.
[47] Fitzpatrick EM, Jones JM, Pourkashanian M, Ross AB, Williams A, Bartle KD. Mechanistic aspects of soot formation from the combustion of pine wood. Energy Fuels 2008;22:3771–8.
[48] Caubet S, Corte P, Fahim C, Traverse JP. Thermochemical conversion of biomass: gasification by flash pyrolysis study. Solar Energy 1982;29:565–72.
[49] Li C, Suzuki K. Tar property, analysis, reforming mechanism and model for biomass gasification—an overview. Renew Sust Energ Rev 2009;13:594–604.
[50] Ledesma EB, Marsh ND, Sandrowitz AK, Wornat MJ. Global kinetic rate parameters for the formation of polycyclic aromatic hydrocarbons from the pyrolyis of catechol, a model compound representative of solid fuel moieties. Energy Fuels 2002;16:1331–6.
[51] Scheer AM, Mukarakate C, Robichaud DJ, Nimlos MR, Ellison GB. Thermal decomposition mechanisms of the methoxyphenols: formation of phenol, cyclopentadienone, vinylacetylene, and acetylene. J Phys Chem A 2011;115:13381–9.
[52] Devi L, Ptasinski KJ, Janssen FJJG. Pretreated olivine as tar removal catalyst for biomass gasifiers: investigation using naphthalene as model biomass tar. Fuel Process Technol 2005;86:707–30.
[53] Swierczynski D, Courson C, Kiennemann A. Study of steam reforming of toluene used as model compound of tar produced by biomass gasification. Chem Eng Process 2008;47:508–13.
[54] Simell PA, Hirvensalo EK, Smolander VT, Krause AOI. Steam reforming of gasification gas tar over dolomite with benzene as a model compound. Ind Eng Chem Res 1999;38:1250–7.
[55] Lv P, Yuan Z, Ma L, Wu C, Chen Y, Zhu J. Hydrogen-rich gas production from biomass air and oxygen/steam gasification in a downdraft gasifier. Renew Energ 2007;32:2173–85.
[56] Abu El-Rub Z, Bramer EA, Brem G. Experimental comparison of biomass chars with other catalysts for tar reduction. Fuel 2008;87:2243–52.
[57] Gilbert P, Ryu C, Sharifi V, Swithenbank J. Tar reduction in pyrolysis vapours from biomass over a hot char bed. Bioresour Technol 2009;100:6045–51.
[58] Jess A. Mechanisms and kinetics of thermal reactions of aromatic hydrocarbons from pyrolysis of solid fuels. Fuel 1996;75:1441–8.
[59] Taralas G, Kontominas MG, Kakatsios X. Modeling the thermal destruction of toluene (C7H8) as tar-related species for fuel gas cleanup. Energy Fuels 2003;17:329–37.
[60] Shie J-L, Chang C-Y, Chen J-H, Tsai W-T, Chen Y-H, Chiou C-S, et al. Catalytic oxidation of naphthalene using a Pt/Al_2O_3 catalyst. Appl Catal B 2005;58:289–97.
[61] Sun Y, Jiang J, Kantarelis E, Xu J, Li L, Zhao S, et al. Development of a bimetallic dolomite based tar cracking catalyst. Catal Commun 2012;20:36–40.
[62] Dou B, Gao J, Sha X, Baek SW. Catalytic cracking of tar component from high-temperature fuel gas. Appl Therm Eng 2003;23:2229–39.
[63] Devi L, Ptasinski KJ, Janssen FJJG, van Paasen SVB, Bergman PCA, Kiel JHA. Catalytic decomposition of biomass tars: use of dolomite and untreated olivine. Renew Energ 2005;30:565–87.
[64] Min Z, Yimsiri P, Asadullah M, Zhang S, Li C-Z. Catalytic reforming of tar during gasification. Part II. Char as a catalyst or as a catalyst support for tar reforming. Fuel 2011;90:2545–52.
[65] Corella J, Orío A, Toledo J-M. Biomass gasification with air in a fluidized bed: exhaustive tar elimination with commercial steam reforming catalysts. Energy Fuels 1999;13:702–9.
[66] Orío A, Corella J, Narváez I. Performance of different dolomites on hot raw gas cleaning from biomass gasification with air. Ind Eng Chem Res 1997;36:3800–8.
[67] Lv P, Yuan Z, Wu C, Ma L, Chen Y, Tsubaki N. Bio-syngas production from biomass catalytic gasification. Energ Convers Manage 2007;48:1132–9.
[68] Narvaez I, Orio A, Aznar MP, Corella J. Biomass gasification with air in an atmospheric bubbling fluidized bed. Effect of six operational variables on the quality of the produced raw gas. Ind Eng Chem Res 1996;35:2110–20.
[69] Fourcault A, Marias F, Michon U. Modelling of thermal removal of tars in a high temperature stage fed by a plasma torch. Biomass Bioenerg 2010;34:1363–74.
[70] Su Y, Luo Y, Chen Y, Wu W, Zhang Y. Experimental and numerical investigation of tar destruction under partial oxidation environment. Fuel Process Technol 2011;92:1513–24.
[71] Zhao B, Zhang X, Chen L, Qu R, Meng G, Yi X, et al. Steam reforming of toluene as model compound of biomass pyrolysis tar for hydrogen. Biomass Bioenerg 2010;34:140–4.
[72] Ji P, Feng W, Chen B. Production of ultrapure hydrogen from biomass gasification with air. Chem Eng Sci 2009;64:582–92.
[73] de Jong W, Ünal Ö, Andries J, Hein KRG, Spliethoff H. Thermochemical conversion of brown coal and biomass in a pressurised fluidised bed gasifier with hot gas filtration using ceramic channel filters: measurements and gasifier modelling. Appl Energy 2003;74:425–37.
[74] Radmanesh R, Chaouki J, Guy C. Biomass gasification in a bubbling fluidized bed reactor: experiments and modeling. AIChE J 2006;52:4258–72.
[75] Barman NS, Ghosh S, De S. Gasification of biomass in a fixed bed downdraft gasifier – a realistic model including tar. Bioresour Technol 2012;107:505–11.
[76] Corella J, Caballero MA, Aznar MP, Brage C. Two advanced models for the kinetics of the variation of the tar composition in its catalytic elimination in biomass gasification. Ind Eng Chem Res 2003;42:3001–11.
[77] Umeki K, Yamamoto K, Namioka T, Yoshikawa K. High temperature steam-only gasification of woody biomass. Appl Energy 2010;87:791–8.
[78] Umeki K, Namioka T, Yoshikawa K. Analysis of an updraft biomass gasifier with high temperature steam using a numerical model. Appl Energy 2012;90:38–45.
[79] Abdelouahed L, Authier O, Mauviel G, Corriou JP, Verdier G, Dufour A. Detailed modeling of biomass gasification in dual fluidized bed reactors under aspen plus. Energy Fuels 2012;26:3840–55.
[80] Norinaga K, Deutschmann O, Saegusa N, Hayashi Ji. Analysis of pyrolysis products from light hydrocarbons and kinetic modeling for growth of polycyclic aromatic hydrocarbons with detailed chemistry. J Anal Appl Pyrol 2009;86:148–60.
[81] Andrae JCG. Comprehensive chemical kinetic modeling of toluene reference fuels oxidation. Fuel 2013;107:740–8.
[82] Norinaga K, Deutschmann O. Detailed kinetic modeling of gas-phase reactions in the chemical vapor deposition of carbon from light hydrocarbons. Ind Eng Chem Res 2007;46:3547–57.
[83] Norinaga K, Sakurai Y, Sato R, Hayashi J-i. Numerical simulation of thermal conversion of aromatic hydrocarbons in the presence of hydrogen and steam using a detailed chemical kinetic model. Chem Eng J 2011;178:282–90.
[84] Norinaga K, Shoji T, Kudo S, Hayashi Ji. Detailed chemical kinetic modelling of vapour-phase cracking of multi-component molecular mixtures derived from the fast pyrolysis of cellulose. Fuel 2013;103:141–50.
[85] Font Palma C. Model for biomass gasification including tar formation and evolution. Energy Fuels 2013, in press. http://dx.doi.org/10.1021/ef4004297..